Available online at www.sciencedirect.com
SCIENCE DIRECT®
Polymer 45 (2004) 399–407
polymer
www.elsevier.com/locate/polymer

Acrylonitrile-based copolymer membranes containing reactive groups: effects of surface-immobilized poly(ethylene glycol)s on anti-fouling properties and blood compatibility

Fu-Qiang Nie[a], Zhi-Kang Xu[a,*], Peng Ye[a], Jian Wu[b,*], Patrick Seta[c]

[a]*Institute of Polymer Science, Zhejiang University, Zheda Lu 38, Hangzhou 310027, People's Republic of China*
[b]*Department of Chemistry, Zhejiang University, Hangzhou 310027, People's Republic of China*
[c]*Institut Européen des Membranes, UMR CNRS no 5635, 34293 Montpellier Cedex 05, France*

Received 4 August 2003; received in revised form 7 November 2003; accepted 11 November 2003

Abstract

The anti-fouling properties and blood compatibility of poly(acrylonitrile-*co*-maleic acid) (PANCMA) membranes were improved by the immobilization of poly(ethylene glycol)s (PEG) on membrane surface. It was found that the reactive carboxyl groups on PANCMA membrane surface could be conveniently conversed into anhydride groups and then esterified with PEG. Chemical and morphological changes as well as biocompatibility on membrane surface were analyzed by Fourier transform infrared spectroscopy, elemental analysis, scanning electron microscopy, water contact angle, protein adsorption, and platelet adhesion. Results revealed that, with the immobilization of PEG, the hydrophilicity and blood compatibility of the acrylonitrile-based copolymer membranes were improved obviously. The molecular weight of PEG had an obvious influence on the properties of the PEG-immobilized membranes. Permeation behaviors for the studied membranes were investigated by water and bovine serum albumin (BSA) filtration experiments. Compared with the original PANCMA membrane, the membrane immobilized with PEG 400 ($M_w = 400$ g/mol) showed a three-fold increase in a BSA solution flux, a 40.4% reduction in total fouling, and a 57.9% decrease in BSA adsorption.

Keywords: Acrylonitrile copolymer membrane; Poly(ethylene glycol); Blood compatibility

1. Introduction

Material surfaces are the phase boundaries that lie between the bulk and the outer environment [1]. The performance of a polymeric material such as separation membrane relies highly upon the properties of the boundaries in many applications because the interactions between the material and environments occur chiefly on its surfaces. Membrane surfaces that show minimal protein adsorption are very important in many regions, not only for ultrafiltration and biosensor but also for blood contacting implant device. Polyacrylonitrile (PAN) and acrylonitrile copolymers have been successfully applied as membrane materials in the fields of dialysis, ultrafiltration, enzyme-immobilization, and pervaporation [2–7]. However, the relatively poor hydrophilicity and biocompatibility for this type of membrane limit their further applications in aqueous solution treatment, enzyme-immobilized membrane bio-reactor, bio-separation and biomedical devices. Increasing the hydrophilicity of the membrane surface can reduce protein fouling and improve biocompatibility for common membranes. Therefore, there are many surface modification methods that have been reported to make ideal hydrophilic and fouling-resistant surfaces. Among them, the grafting of hydrophilic monomers on membrane surface shows some promise [8–12]. However, conventional processes require a prefunctionalization step to introduce some reactive groups on the membrane surface for covalent grafting. Irradiation methods with plasma, electron beam, γ-ray and ultra-violet light have been widely used [13]. In some cases, irradiation may do some damage to the membranes exposed to energy sources such as electron beam and γ-ray, which may alter the bulk properties of the membranes and limit their applications.

* Corresponding author. Tel.: +86-571-87952605; fax: +86-571-87951773.
E-mail address: xuzk@ipsm.zju.edu.cn (Z.K. Xu).

0032-3861/$ - see front matter © 2003 Elsevier Ltd. All rights reserved.
doi:10.1016/j.polymer.2003.11.007

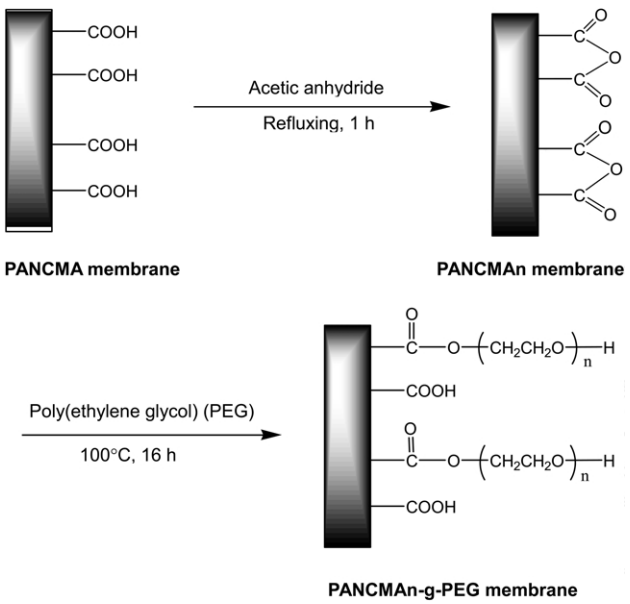

Fig. 1. Fabrication process for the acrylonitrile-based copolymer membranes studied in this work.

In order to accomplish the objective mentioned above, it may be also one effective way to copolymerize acrylonitrile with vinyl monomers containing reactive groups such as maleic anhydride to gain prefunctionalization on membrane surface. These anhydride groups can easily undergo a ring opening reaction with nucleophilic reagents which contain hydroxyl or amine groups. For examples, styrene/maleic anhydride copolymers had been reacted with poly(ethylene glycol) (PEG) to synthesize amphiphilic graft copolymers with thermo-sensitive and/or pH-sensitive properties [14,15]. In our previous work [16], ultrafiltration hollow fiber membranes containing reactive groups were fabricated from poly(acrylonitrile-*co*-maleic acid)s (PANCMA) which were synthesized by water-phase precipitation copolymerization with main advantages including high molecular weight, high monomer conversion, and environmental friendship. Moreover, it had been confirmed that the reactive carboxyl groups on membrane surface can be easily conversed into anhydride groups and then reacted with PEG. The objective of this study is to improve the anti-fouling properties and blood compatibility by immobilizing PEG on the surface of PANCMA membranes. PEG is well known for its extraordinary ability to resist protein adsorption because of its hydrophilicity, large excluded volume, and unique coordination with surrounding water molecules in an aqueous medium. Furthermore, it is found that the extent of protein rejection is related to PEG molecular weight and graft density on membrane surface [17–19]. Therefore, as representatively shown in Fig. 1, poly(acrylonitrile-*co*-maleic anhydride) (PANCMAn) membranes were obtained by refluxing the corresponding PANCMA membranes in acetic anhydride. A series of PEG with different molecular weight were immobilized on the PANCMAn membrane surface by the esterification reaction of the reactive anhydride groups. After immobilizing PEG on the membranes surface, the virgin and modified membranes were compared with respect to their hydrophilicity, platelet adhesion, protein adsorption, water and protein solution permeation as well as the flux recovery after BSA solution filtration by water and chemical cleaning.

2. Experimental

2.1. Materials

All chemicals were analytical grade. The acrylonitrile/-maleic acid copolymer containing 3.69 mol% of maleic acid (PANCMA, $M_w = 15.8 \times 10^4$ g/mol) were synthesized in our laboratory. Dimethyl sulfoxide (DMSO) was purified by vacuum distillation before used. Bovine serum albumin (BSA, purity >98%) was purchased from Sino-American Biotechnology Co. and used as received. A total of 0.1 wt% BSA solution was prepared in a phosphate buffered saline (PBS) solution at pH 7.4. The molecular weights of the poly(ethylene glycol)s ranged from 200 to 1000 g/mol, and were used as received. The nonsolvent selected for the coagulation bath for fabricating microporous membrane was ultrafiltrated water, while deionized water was used for the filtration experiment.

2.2. Preparation of membranes

PANCMA was used as membrane material. This polymer were dried for at least 3 h at 50 °C in vacuum oven, and then dissolved in DMSO at about 80 °C for 24 h with vigorous stirring to form a homogenous 4 wt% casting solution. After removing air bubble, the casting solution was cast onto a clean glass plate using a casting knife with 100 μm gate opening. To fabricate microporous membrane, the nascent membrane was placed in the air (25 ± 1 °C, 45–50% relative humidity) for 10 min, and then immersed in 22 ± 1 °C ultrafiltrated water for 24 h. On the other hand, the nascent membrane was dried in an oven at 120 °C for 3 h to obtain dense membrane. These membranes were used for different experiments. All microporous membranes were preserved in 5 vol% formaldehyde solutions for further use.

2.3. Grafting PEG on membranes

PANCMA membrane was first washed with a water–ethanol–hexane sequence, and dried at room temperature. To transfer the reactive groups on the membrane surface from carboxyls to anhydrides, the dry membrane of PANCMA was refluxed in acetic anhydride for 1 h to ensure a high conversion [20]. Then the membrane was thoroughly washed with acetone and completely dried at 40 °C in vacuum oven for 3 h, which was marked as PANCMAn membrane.

The dry PANCMAn membrane was immersed in PEG at

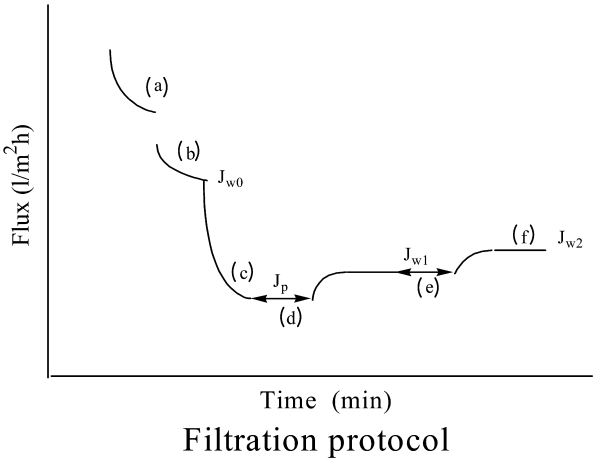

Fig. 2. Filtration protocol. (a) compaction step; (b) deionized water filtration step; (c) BSA solution filtration step; (d) deionized water cleaning step; (e) chemical cleaning step; (f) deionized water cleaning step. J_{w0}, initial deionized water flux; J_p, 1 g/l BSA solution flux; J_{w1}, deionized flux after water cleaning; J_{w2}, deionized water flux after chemical cleaning.

100 °C under nitrogen atmosphere for about 16 h [21,22]. The resulted membrane was washed using large amount of deionized water to remove unreacted PEG. It was then dried completely at 40 °C in vacuum oven. The obtained membranes were designated as PANCMAn-*g*-PEG200, PANCMAn-*g*-PEG400, PANCMAn-*g*-PEG600, and PANCMAn-*g*-PEG1000, respectively, with each number referring the molecular weight of PEG. The grafting degree (DG) was calculated by the following equation

$$\mathrm{DG}(\%) = \frac{w_g - w_0}{w_0} \times 100$$

where w_0 and w_g are the weight of a membrane before and after grafting reaction, respectively.

2.4. Fourier transform infrared spectroscopy

In order to investigate the chemical changes between the original and PEG-immobilized dense membranes and confirm the immobilization of PEG on membrane surface, Fourier transform infrared spectroscopy (FT-IR, Vector 22) with an ATR unit (KRS-5 crystal, 45°) was used.

2.5. Elemental analysis

Elemental analysis was used to detect the atomic composition of the original and PEG-immobilized membranes. The weight percent of carbon, hydrogen and nitrogen of each sample was obtained from an elemental analyzer (EA1110, Carco Erba Co., Italy), and then that of oxygen was calculated from EA data.

2.6. Hydrophilicity measurements

The hydrophilicity of the membrane surface was characterized on the basis of pure water contact angle and water absorbance measurements. Using a sessile drop method, water contact angle was measured at room temperature on a contact angle goniometer (KRÜSS DSA10-MK) equipped with video capture. A total of 1 μl of deionized water was dropped onto a dry dense membrane with a micro syringe in an atmosphere of saturated water vapor. At least 10 contact angles were averaged to get a reliable value. Water absorbance was defined as $(w_2 - w_1)/s$, where w_1 and w_2 represent the weight of dried membrane and the membrane soaked in water for 24 h at 22 ± 0.5 °C, respectively, and s is the effective area of the tested membrane. The reported values were the mean of at least ten experiments and the standard deviation was within ca ± 2%.

2.7. Scanning electron microscopy

The surface morphologies of the original and PEG-modified membranes were examined by scanning electron microscopy (SEM) using a CAMBRIDGE S-260 Scanning Microscope. For this purpose, membrane samples were washed with a water–ethanol–hexane sequence and dried at room temperature, and then coated with a 20 nm gold layer before SEM analysis.

2.8. Filtration experiments

The filtration protocol, which is shown in Fig. 2, was similar to that of Pieracci et al. [9,10]. Each membrane was first compacted for 30 min at 0.15 MPa. Then, the pressure was lowered to 0.10 MPa and the flux of deionized water (J_{w0}) was measured by weighing permeate until consecutive recorded values differed by less than 2% (J_0). Next, a 1 g/l BSA solution was added to the reservoir and the filtering experiment was performed at 0.10 MPa for 30 min, the permeate flux at the end of BSA solution filtration was denoted as J_p. After BSA solution filtration, the membrane was cleaned for 1 min three times to remove weakly attached BSA, and then the deionized water flux (J_{w1}) was measured at 0.10 MPa. The membrane was filled with a 500 ppm NaOCl solution and filtered for 1 h at 0.10 MPa. Thereafter, the membrane was cleaned with deionized water, and the additional filtering of deionized water was performed for 20 min in order to completely remove the remaining NaOCl. The next measured deionized water flux was J_{w2}. The reported data was the mean value of triplicate samples for each membrane.

The amount of adsorbed BSA that had not been removed after chemical cleaning was determined by measuring the weight of the membrane before and after the filtration experiment, which was completely dried and stored in a desiccator under nitrogen purge.

2.9. Adhesion of blood platelet

Fresh platelet-rich plasma (PRP), which was obtained

Table 1
Elemental analysis data for the studied membranes

Sample no	Nitrogen (wt%)	Carbon (wt%)	Hydrogen (wt%)	Oxygen (wt%)
PANCMA	25.12	64.88	5.61	4.40
PANCMAn	25.38	65.56	5.49	3.47
PANCMAn-*g*-PEG200	22.84	63.97	5.82	7.28
PANCMAn-*g*-PEG400	21.04	63.31	6.13	9.53
PANCMAn-*g*-PEG600	19.98	62.89	6.28	10.85
PANCMAn-*g*-PEG1000	18.79	62.47	6.44	12.29

from 20 ml of human fresh blood by centrifuged at 1000 rpm for 10 min, was used in all experiments. The studied dense flat membranes was cut into 1×1 cm^2 pieces and placed in tissue culture plates. 20 μl fresh PRP was dropped on the center of the membrane samples and then incubated at 22 ± 0.5 °C for 30 min. The membranes were rinsed gently with a phosphate buffered saline (PBS) solution, after which the adhered platelets were fixed with 2.5 wt% glutaraldehyde in PBS for 30 min. Finally, the samples were washed with PBS, dehydrated with a series of ethanol/water mixtures of increasing ethanol concentration (30, 40, 50, 60, 70, 80, 90, 100% ethanol, 10 min in each mixture) [23,24]. The surface of each membrane was coated with gold and observed with SEM.

3. Results and discussion

Fig. 3 shows the FT-IR/ATR spectra of the original and PEG-immobilized membranes. It can be seen that the spectrum of PANCMA membrane (Fig. 3(a)) showed an absorbance band at 1725 cm^{-1}, which was the characteristic band for carboxyl group. Conversing carboxyl into anhydride could be confirmed by the appearance of two absorbance bands at 1785 and 1825 cm^{-1} (Fig. 3(b)). Compared with the spectrum of PANCMAn, on the other hand, the characteristic bands of anhydride disappeared in the spectrum of PANCMAn-*g*-PEG (Fig. 3(c)–(f)), while the 1716 cm^{-1} for C=O stretching vibration of the ester group appeared. Furthermore, the intensity of 1060 cm^{-1} band for C–O stretching vibration enhanced slightly with the molecular weight and immobilizing density of PEG on membrane surface. PEG immobilization on PANCMAn membranes were also demonstrated by elemental analysis and grafting degree determination. The weight percentage of nitrogen, carbon, hydrogen and oxygen of the studied membranes and the grafting degree are summarized in Tables 1 and 2, respectively. Although the grafting degree increased from 9.97 to 25.49% for PANCMAn-*g*-PEG200 to PANCMAn-*g*-PEG1000, it was found on the basis of calculated immobilization density that, with the molecular weight of PEG increasing from 200 to 1000 g/mol, the immobilization of PEG on PANCMAn membrane surface was relatively difficult to take place.

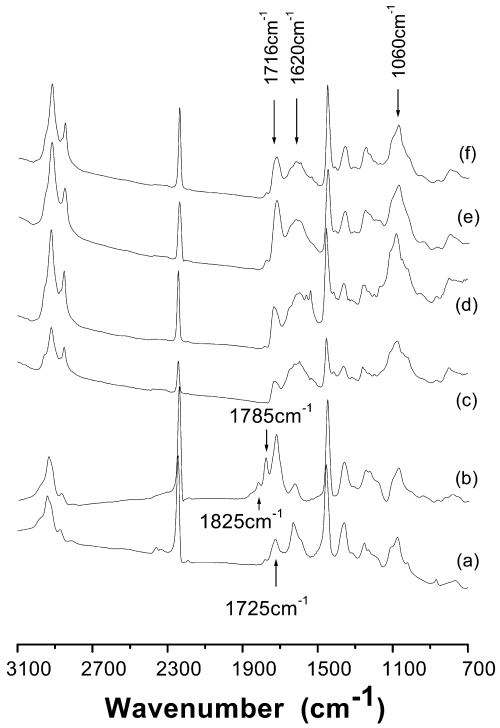

Fig. 3. FT-IR/ATR spectra of the original and PEG-immobilized membranes. (a) PANCMA; (b) PANCMAn; (c) PANCMAn-*g*-PEG200; (d) PANCMAn-*g*-PEG400; (e) PANCMAn-*g*-PEG600; (f) PANCMAn-*g*-PEG1000.

Table 2
Characteristics of the original and PEG-immobilized membranes

Membrane	Grafting degree[a] (%)	Immobilization density[b] (mol/cm^2)	Water absorption[c] ($\times 10^{-3}$ g/cm^2)	Contact angle[d] (°)
PANCMA	–	–	12.05	48.2 ± 0.2
PANCMAn	–	–	9.93	57.2 ± 0.1
PANCMAn-*g*-PEG200	9.97	1.12×10^{-5} (2.24)[e]	20.38	31.4 ± 0.3
PANCMAn-*g*-PEG400	16.52	5.93×10^{-6} (2.37)	26.62	23.1 ± 0.2
PANCMAn-*g*-PEG600	21.27	4.12×10^{-6} (2.47)	21.58	34.3 ± 0.1
PANCMAn-*g*-PEG1000	25.49	2.56×10^{-6} (2.56)	18.65	39.1 ± 0.4

[a] $((w_g - w_0)/w_0) \times 100$, w_0 and w_g represent the weight of membrane before and after the reaction.
[b] Calculated from the grafting degree and the membrane area.
[c] $(w_2 - w_1)/s$, w_1 and w_2 represent the weight of dried membrane and the membrane soaked in water for 24 h, s is the effective membrane area.
[d] Measured by sessile drop method.
[e] Unit for the value in bracket is mg/cm^2.

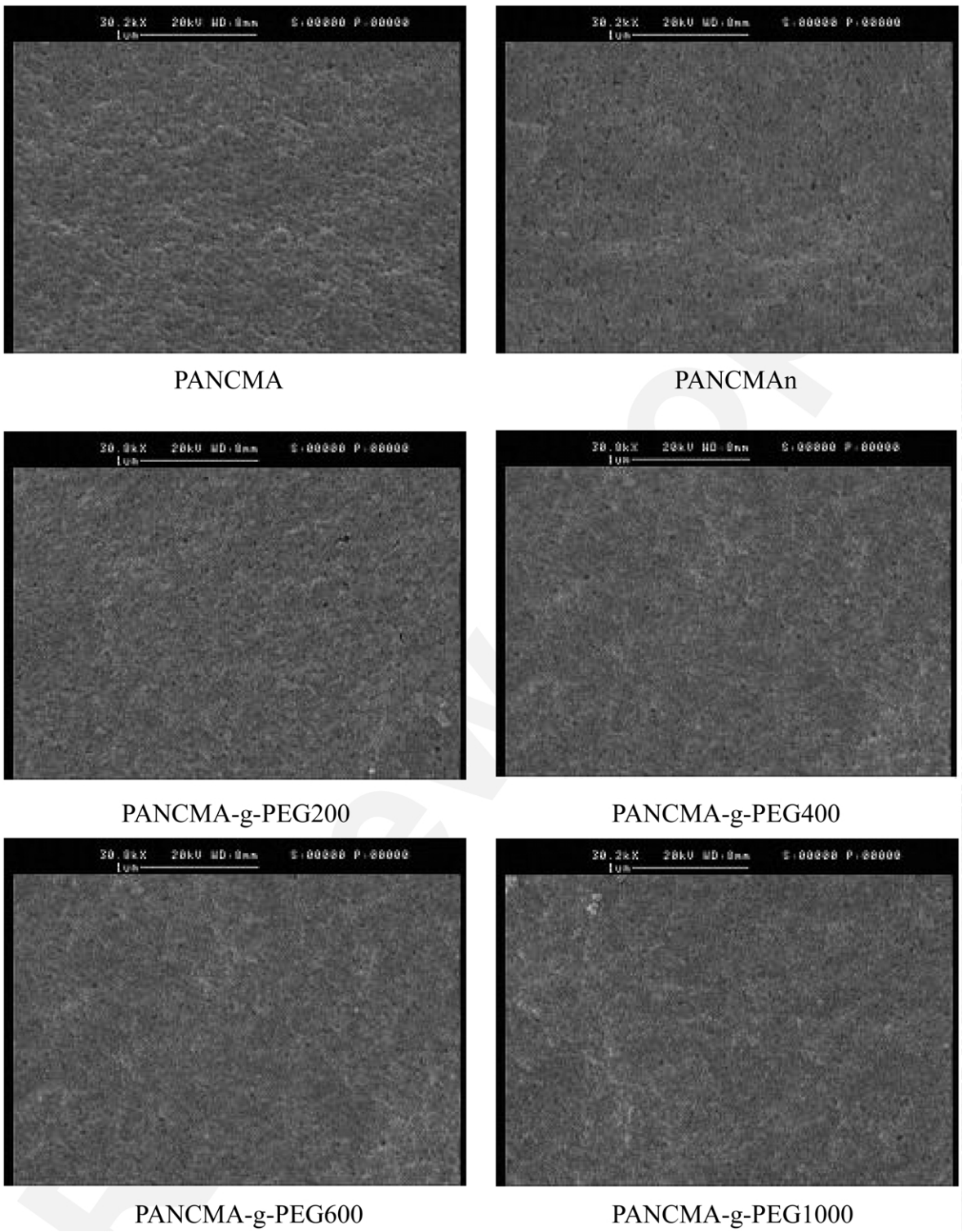

Fig. 4. SEM photographs of the original and PEG-immobilized membranes surface.

The morphological changes of the original and PEG-immobilized membranes were examined with SEM at a magnification of 30,000. Typical pictures are shown in Fig. 4. It seems that both pore number and pore size on membrane surface decreased slightly with the immobilization of PEG.

Water contact angle and water absorbance have been commonly used to characterize the relative hydrophilicity or hydrophobicity of membrane surface. Static water contact angles for the studied membranes are summarized in Table 2. It can be seen that all PEG-immobilized membranes showed lower contact angles than those of PANCMA and PANCMAn. Among them, PANCMAn-*g*-PEG400

Table 3
Permeation fluxes of de-ionized water and BSA solution through the original and PEG-immobilized membranes

Membrane	J_{w0} (l/m^{2}h)	J_p (l/m^{2}h)	J_{w1} (l/m^{2}h)	J_{w2} (l/m^{2}h)	BSA (mg/g)[a]
PANCMA	303.3 ± 15.2	112.7 ± 5.7	138.6 ± 6.8	168.0 ± 5.8	7.61 ± 0.23
PANCMAn	277.3 ± 11.1	98.3 ± 3.9	113.0 ± 4.8	138.8 ± 6.2	9.31 ± 0.19
PANCMAn-*g*-PEG200	372.6 ± 22.3	197.6 ± 5.9	249.0 ± 9.8	280.0 ± 11.6	4.72 ± 0.18
PANCMAn-*g*-PEG400	519.9 ± 20.8	325.3 ± 16.3	385.3 ± 18.1	443.3 ± 12.8	3.20 ± 0.16
PANCMAn-*g*-PEG600	450.6 ± 13.5	253.2 ± 12.7	309.3 ± 15.2	339.0 ± 10.2	3.43 ± 0.10
PANCMAn-*g*-PEG1000	311.9 ± 15.6	150.6 ± 6.0	193.9 ± 8.6	222.5 ± 7.6	3.66 ± 0.15

The filtration test was conducted at a constant transmembrane pressure of 0.1 MPa and a system temperature of 22 ± 1 °C. Error range, ±5%.
[a] The amount of absorbed BSA on the membrane after chemical cleaning.

membrane manifested the lowest value of 23.1 ± 0.2° which was a half of that for PANCMA membrane. However, with the molecular weight of PEG increasing from 400 to 1000, the contact angle of PEG-immobilized membrane increased again from 23.1 to 39.1°. Water absorbance data listed in Table 2 also had a similar trend as contact angle, since more hydrophilic surface was more easily to absorb water. These results indicated that the hydrophilicity of PANCMA membrane surface was effectively improved by the immobilization of PEG chains, and the molecular weight of PEG had an obvious effect. As shown in Table 2, although PANCMAn-*g*-PEG200 membrane had the highest immobilization density, the short PEG chain with less hydrophilic $-CH_2-CH_2-O-$ segment brought about relatively low hydrophilicity on membrane surface than that of PANCMAn-*g*-PEG400. On the other hand, PEG600 and PEG1000 were more difficult to be immobilized on membrane surface, therefore, the hydrophilicity of the resultant membrane decreased also. In order to obtain an optimal hydrophilicity, a moderate molecular weight of PEG might be better due to its balance of immobilization density and hydrophilic chain segments.

To investigate the performances of the studied membranes, deionized water and BSA solution filtration experiments were carried out. Typical results for the permeation fluxes of deionized water and BSA solution through PANCMA, PANCMAn and PEG-immobilized membranes are depicted in Table 3. The symbols, J_{w0} and J_p were defined as the flux of deionized water and BSA solution, respectively. As shown in Table 3, although both pore number and pore size on membrane surface decreased from PANCMAn-*g*-PEG200 to PANCMAn-*g*-PEG1000 as observed by SEM, PEG-immobilized membranes had higher permeation values than those of PANCMA and PANCMAn. Again, PANCMAn-*g*-PEG400 had the best filtration properties among all studied membranes. Compared with PANCMA and PANCMAn, PANCMAn-*g*-PEG400 showed almost a two-fold increase in J_{w0} and a three-fold increase in J_p. However, compared with that of PANCMAn-*g*-PEG400, the J_{w0} and J_p of PANCMAn-*g*-PEG600 and PANCMAn-*g*-PEG1000 membranes decreased because high molecular weight PEG led to relatively low hydrophilicity and small pores on membrane surface as mentioned above.

The effects of deionized water cleaning and chemical

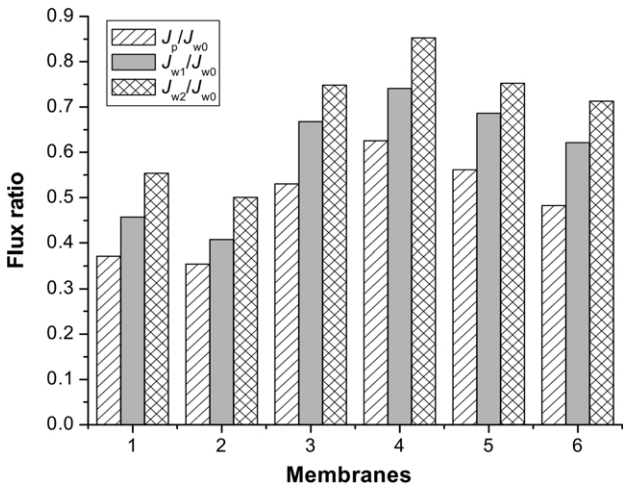

Fig. 5. Effect of deionized water cleaning and chemical cleaning on the flux ratios of the original and PEG-immobilized membranes. (1) PANCMA; (2) PANCMAn; (3) PANCMAn-*g*-PEG200; (4) PANCMAn-*g*-PEG400; (5) PANCMAn-*g*-PEG600; (6) PANCMAn-*g*-PEG1000.

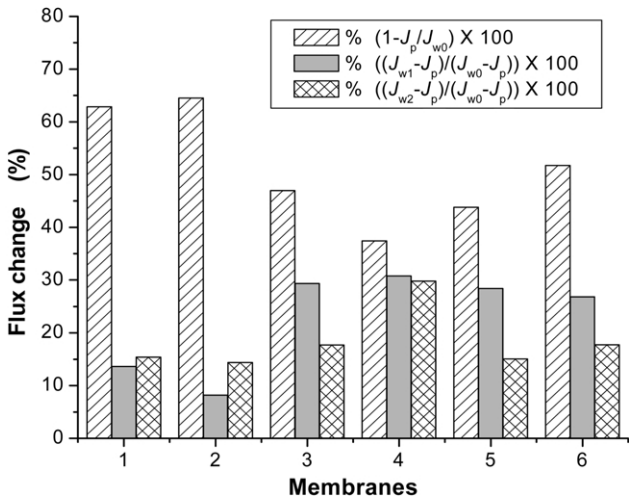

Fig. 6. Flux changes of the original and PEG-immobilized membranes during filtration and after water and chemical cleaning in detail. Total fouling: $(1 - J_p/J_{w0}) \times 100$; flux recovery by water cleaning: $((J_{w1} - J_p)/(J_{w0} - J_p)) \times 100$; flux recovery by chemical cleaning: $((J_{w2} - J_{w1})/(J_{w0} - J_p)) \times 100$. (1) PANCMA; (2) PANCMAn; (3) PANCMAn-*g*-PEG200; (4) PANCMAn-*g*-PEG400; (5) PANCMAn-*g*-PEG600; (6) PANCMAn-*g*-PEG1000.

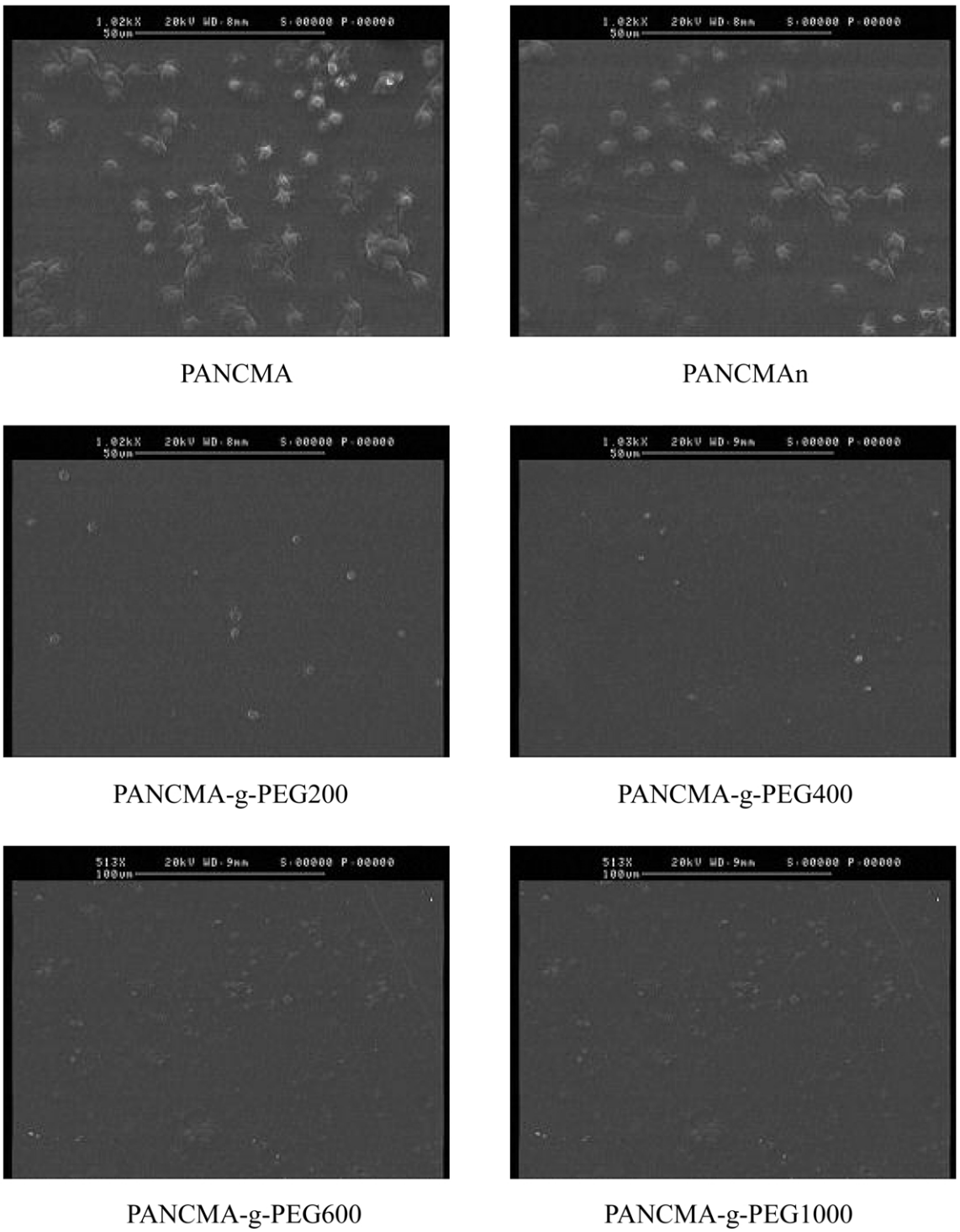

Fig. 7. Adhesion of blood platelets on the surface of original and PEG-immobilized dense membrane.

cleaning on the membrane filtration performances are shown in Fig. 5. In this figure, the relative ratios of BSA solution permeation flux (J_p), water permeation flux after water cleaning (J_{w1}), and water permeation flux after chemical cleaning (J_{w2}) to water permeation flux (J_{w0}) are presented. It was found that the J_p/J_{w0}, J_{w1}/J_{w0} and J_{w2}/J_{w0} of the membranes increased from PANCMAn-*g*-PEG200 to PANCMAn-*g*-PEG400, and then decreased slowly from PANCMAn-*g*-PEG400 to PANCMAn-*g*-PEG1000. However, all PEG-immobilized membranes showed higher values than those of PANCMA and PANCMAn. It should be noticed that J_{w2}/J_{w0} for PANCMAn-*g*-PEG400 membrane was 0.85, which meant that the filtration performance of this membrane was more effectively recovered by water

cleaning and chemical cleaning. Fig. 6 shows the percent of total fouling ($(1 - J_p/J_{w0}) \times 100$), the flux recovery by water cleaning ($(J_{w1} - J_p)/(J_{w0} - J_p) \times 100$), and the flux recovery by chemical cleaning ($(J_{w2} - J_{w1})/(J_{w0} - J_p) \times 100$) for the membranes [9,10]. It was found that the total fouling decreased from 62.68% for PANCMA to 37.44% for PANCMAn-*g*-PEG400. Concerning $((J_{w1} - J_p)/(J_{w0} - J_p)) \times 100$ and $((J_{w2} - J_{w1})/(J_{w0} - J_p)) \times 100$, each PEG-immobilized membrane showed higher values in comparison with PANCMA and PANCMAn membranes. These data demonstrated that when the adsorption of protein took place on the surface of PEG-immobilized membranes, the proteins were removed easily by deionized water and chemical cleaning. All these results indicated clearly that fouling caused by the adsorption of BSA could be efficiently reduced with the immobilization of PEG on the surface of acrylonitrile copolymer-based membranes.

From Table 3, it can also be seen that the amount of adsorbed BSA remained on membrane surface after chemical cleaning decreased obviously with the immobilization of PEG. PANCMAn-*g*-PEG400 membrane had a lowest adsorption value and it reduced about 57.9% comparing with PANCMA. It had been generally thought the prevention of protein adsorption was mainly due to the steric repulsion by the surface-grafted PEG chains [24,25]. Fig. 7 shows the situation of platelets adhering on the PANCMA, PANCMAn, and PEG-immobilized membranes surface from platelets-rich plasma (PRP). When a material contacted with blood, proteins were first adsorbed instantaneously on surfaces and deformed, then platelets were adsorbed, activated, and aggregated so that platelets played a major role in the thrombus formation. Therefore, a study on platelets adhesion to evaluate the blood compatibility of separation membrane was important. It can be seen obviously from Fig. 7 that many platelets adhered on the PANCMA and PANCMAn membranes. On the other hand, platelets were rarely observed on PEG-immobilized membranes. It was well accepted that PEG had a unique nonadhesive property to blood components, the specific character of PEG was explained by the excluded volume effect and the dynamic motion of fully hydrated flexible chains [25]. The SEM pictures shown in Fig. 7 revealed that the blood compatibility of the membrane was improved highly by immobilizing PEG chains on membrane surface. This result was in full agreement with the literatures [25,26]. Moreover, PANCMAn-*g*-PEG400 had the best blood compatibility than other PEG-immobilized membranes, because protein adsorption was the first step for platelets to adhere and PANCMAn-*g*-PEG400 was the most effective membrane to prevent protein adsorption.

4. Conclusions

Through the esterification reaction of anhydride groups on the surfaces of PANCMAn membrane with hydroxyl end groups in PEG, PEG could be immobilized on membrane surface. Both water contact angle and water adsorption measurements demonstrated that the hydrophilicity of the membranes was improved by PEG immobilization. The permeation flux of water and BSA solution for the PEG-immobilized membranes increased due to the enhancement of hydrophilicity on membrane surface. The flux recovery of the PEG-immobilized membranes after water and chemical cleaning was superior to that of original PANCMA and PANCMAn membranes. Compared with PANCMA membrane, membrane modified with PEG 400 ($M_w = 400$) showed the best performance derived from a three-fold increase in a BSA solution flux, a 40.4% reduction in total fouling, and a 57.9% decrease in BSA adsorption. All PEG-immobilized membranes manifested better blood compatibility than that of PANCMA and PANCMAn membranes. As a conclusion, the reported PEG immobilization method was effective to improve the anti-fouling properties and blood compatibility of acrylonitrile-based copolymer membranes.

Acknowledgements

The financial supports of the National Nature Science Foundation of China (Grant no 50273032) and the High-Tech Research and Development Program of China (Grant no 2002AA601230) are gratefully acknowledged.

References

[1] Kato K, Uchida E, Kang ET, Uyama Y, Ikada Y. Prog Polym Sci 2003;28:209.
[2] Bhat AA, Pangarkar VG. J Membr Sci 2000;167:187.
[3] Trotta F, Drioli E, Baggiani C, Lacopo D. J Membr Sci 2002; 201:77.
[4] Broadhead KW, Tresco PA. J Membr Sci 1998;147:235.
[5] Godjevargova T, Konsulov V, Dimov A, Vasileva N. J Membr Sci 2000;172:279.
[6] Hicke H-G, Lehmann I, Malsch G, Ulbricht M, Becker M. J Membr Sci 2002;198:187.
[7] Musale DA, Kulkarni SS. J Membr Sci 1997;136:13.
[8] Zeman LJ, Zydney A. Microfiltration and ultrafiltration: principles and applications. New York: Marcel Dekker; 1996.
[9] Pieracci J, Crivello JV, Belfort G. Chem Mater 2002;14:256.
[10] Pieracci J, Crivello JV, Belfort G. J Membr Sci 1999;156:223.
[11] Ma H, Bowman CN, Davis RH. J Membr Sci 2000;173:191.
[12] Higuchi A, Shirano K, Harashima M, Yoon BO, Hara M, Hattori M, Imamura K. Biomaterials 2002;23:2659.
[13] Tseng Y-C, McPherson T, Yuan CS, Park K. Biomaterials 1995;16: 963.
[14] Yin X, Stöver HDH. Macromolecules 2002;35:10178.
[15] Hou S-S, Kou P-L. Polymer 2001;42:2387.
[16] Nie F-Q, Xu Z-K, Ming Y-Q, Kou R-Q, Liu Z-M, Wang S-Y. Desalination 2003; in press.
[17] Jo S, Park K. Biomaterials 2000;21:605.
[18] Ulbricht M, Matuschewski H, Oechel A, Hicke HG. J Membr Sci 1999;115:31.

[19] Tziampazis E, Kohn J, Moghe P. Biomaterials 2000;21:511.
[20] Liu XQ, Jikei M, Kakimoto M. Macromolecules 2001;34:3146.
[21] Oh SJ, Jung JC, Zin WC. J Colloid Interf Sci 2001;238:43.
[22] Lin YS, Hlady V, Golander CG. Colloids Surf B 1994;3:49.
[23] Wetzels GMR, Koole LH. Biomaterials 1999;20:1879.
[24] Higuchi A, Shiranoa K, Harashimaa M, Yoona BO, Haraa M, Hattorib M, Imamura K. Biomaterials 2002;23:2659.
[25] Ko YG, Kim YH, Park KD, Lee HJ, Lee WK, Park HD, Kim SH, Lee GS, Ahn DG. Biomaterials 2001;22:2115.
[26] Klee D, Höcker H. Adv Polym Sci 2000;149:1.